

# *Electrodeposition of catalytically active Co-Ni-Tl alloy powders from dilute sulphate baths*

A. M. ABD EL-HALIM

*Department of Chemistry, Faculty of Science, Ain Shams University, Cairo, Egypt*

R. M. KHALIL

*Department of Chemistry, Faculty of Science, King Abdulaziz University, Jeddah, Saudi Arabia*

Received 13 November 1986; revised 23 December 1986

---

Cobalt-nickel-thallium alloy powders were electrodeposited from dilute metal sulphate baths of composition:  $0.007\text{--}0.0245\text{ mol l}^{-1}$   $\text{CoSO}_4 \cdot 7\text{H}_2\text{O}$ ,  $0.0245\text{--}0.007\text{ mol l}^{-1}$   $\text{NiSO}_4 \cdot 6\text{H}_2\text{O}$ ,  $0.001\text{ mol l}^{-1}$   $\text{TlCl}$ ,  $0.5\text{ mol l}^{-1}$   $(\text{NH}_4)_2\text{SO}_4$ ,  $0.07\text{ mol l}^{-1}$   $\text{Na}_2\text{SO}_4 \cdot 10\text{H}_2\text{O}$  and  $0.4\text{ mol l}^{-1}$   $\text{H}_3\text{BO}_3$ . The cathodic polarization curves were traced during electrodeposition and utilized in the discussion of a reaction mechanism for the electrolytic powder deposition. The alloy composition and the cathodic current efficiency were influenced to a great extent by the bath composition (I) and slightly by the deposition current density (II). Irrespective of variables (I) and (II), the electrodeposition of the alloy belonged to the anomalous type. The surface morphology and the catalytic activity, towards the decomposition of 0.4%  $\text{H}_2\text{O}_2$  solution, of the as-deposited alloy powders were affected predominantly by the percentage of cobalt in the alloy. X-ray diffraction studies showed that the alloys consisted mainly of the face-centred cubic nickel phase either alone or with minor proportions of face-centred cubic cobalt phase and hexagonal close-packed  $\alpha$ -cobalt phase. The occurrence of the latter phases was observed only in the alloys with a higher cobalt percentage than nickel.

---

## **1. Introduction**

Recently, we have undertaken research on the electrodeposition of fine-grained and catalytically active metal and alloy powders from dilute metal sulphate solutions within the range found in some industrial effluents. An earlier publication [1] dealt with the electrodeposition of thallium powder because of its importance as a grain refiner in electrodeposited alloys [2].

Detailed studies were focused on finding the optimum bath composition for nickel powder deposition [3] and examining the influence of the operating conditions on the characteristics of the electrodeposited nickel powder [4]. The results have shown that the current efficiency is relatively low and the electrodeposited nickel powder has a moderate catalytic activity towards the decomposition of 0.4%  $\text{H}_2\text{O}_2$  solution. As expected, the codeposition of thallium with nickel improved the catalytic activity and

current efficiency of the electrodeposited nickel-thallium alloy powder [5]. In addition, further work has examined the influence of the operating conditions on the characteristics of the electrodeposited nickel-thallium alloy powder [6].

For reasons of economy we preferred using another alloying metal more conventional in industry and cheaper than thallium. Consequently, due to the similarity in the electrochemical behaviour of cobalt and nickel, an intensive investigation has been made of the electrodeposition of cobalt powder from a bath corresponding in composition to that for nickel deposition [7]. The cobalt powder was deposited with a higher current efficiency and had a markedly higher catalytic activity than nickel. Therefore, our interest was extended to electrodeposition of cobalt-nickel alloy powder [8]. The latter alloy was characterized by higher current efficiency and catalytic activity

than either unalloyed nickel or nickel-thallium alloy powders.

The present study concerns the electrodeposition of cobalt-nickel-thallium alloy powder and is a logical continuation of the above-mentioned investigations.

## 2. Experimental details

A series of baths used for electrodeposition of the ternary cobalt-nickel-thallium alloy powder was selected within the optimum range of bath composition suitable for electrodeposition of the individual constituent metals [1, 3, 7] and some of their binary alloys [5, 8]. These baths were freshly prepared in distilled water using AnalaR chemicals (BDH) and their compositions are given in Table 1. The as-prepared baths have almost the same pH (4.7) and specific conductance ( $0.07 \Omega^{-1} \text{cm}^{-1}$ ). The composition of the baths was varied in a systematic way in which the total metal content (0.0255 M) and the metal-percentage of thallium (12.4%) were held constant and the ratio of cobalt to nickel changed gradually. The composition of the deposit then became a function of the metal-percentage of either cobalt or nickel in the bath.

The experimental arrangement for the electrodeposition process consisted of a Perspex cell fitted with a copper cathode positioned midway between two plane-parallel platinum anodes; all electrodes were of the same geometrical area ( $2.5 \times 3.0 \text{ cm}$ ). During electrodeposition the anodes were surrounded by asbestos diaphragms to preclude oxidation of the  $\text{Co}^{2+}$  and  $\text{Tl}^+$  ions and to avoid errors in the measured potentials caused by oxygen liberated at the anodes.

The polarization curves, relative to the satu-

rated calomel electrode (SCE), were determined with a Wenking potentiostat model POS 73 and recorded automatically by means of a Philips x-y recorder model PM 8132. The composition of each electrodeposited alloy was determined by means of a Perkin-Elmer atomic absorption spectrophotometer model 5000. The cathodic current efficiency ( $f$ ) was determined by using a standard copper coulometer. The morphology of the as-deposited powders was examined with a scanning electron microscope (JEOL model JSM 35). X-ray diffraction studies were carried out using a Philips X-ray diffractometer PW 1390, with a nickel filter and copper radiation. The percentage decomposition ( $D$ ) of 0.4%  $\text{H}_2\text{O}_2$  solution (at  $40^\circ \text{C}$ ) on the surface of the electrodeposited powders was considered as a measure of their catalytic activity. Therefore, a definite volume (50 ml) of the  $\text{H}_2\text{O}_2$  solution was passed (single pass) over a fixed bed (0.15 g) of the test powder with a constant flow-through rate ( $150 \text{ ml h}^{-1}$ ) by means of a peristaltic pump (LKB Bromma model 3132). Values of  $D$  were calculated by measuring the exact concentrations of  $\text{H}_2\text{O}_2$  spectrophotometrically before and after its passage over the powder. Unless otherwise stated all types of measurements were carried out at  $25^\circ \pm 1^\circ \text{C}$ .

## 3. Results and discussion

### 3.1. Polarization curves

The cathodic polarization curves for the electrodeposition of cobalt-nickel-thallium alloy powders from baths 1 to 5 are shown in Fig. 1a. The curves exhibit the same general features and are characterized by an initial rapid potential shift in the negative direction followed by a

Table 1. Composition of the examined alloy deposition baths (pH = 4.7)

Bath number	Concentration in bath ( $\text{mol l}^{-1}$ )					
	$\text{CoSO}_4 \cdot 7\text{H}_2\text{O}$	$\text{NiSO}_4 \cdot 6\text{H}_2\text{O}$	$\text{TlCl}$	$(\text{NH}_4)_2\text{SO}_4$	$\text{Na}_2\text{SO}_4 \cdot 10\text{H}_2\text{O}$	$\text{H}_3\text{BO}_3$
1	—	0.0245	0.0010	0.50	0.070	0.40
2	0.0070	0.0175	0.0010	0.50	0.070	0.40
3	0.0120	0.0125	0.0010	0.50	0.070	0.40
4	0.0175	0.0070	0.0010	0.50	0.070	0.40
5	0.0245	—	0.0010	0.50	0.070	0.40

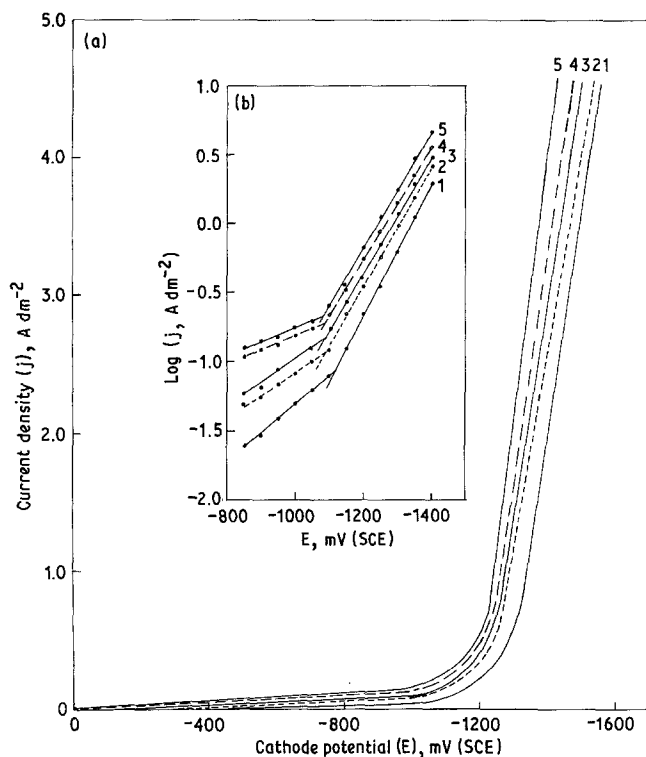


Fig. 1. (a) Polarization curves and (b) Tafel lines for electrodeposition of alloy powders from baths 1 to 5.

gradual increase with rise of current density. These data indicate that the electrodeposition process is attended by large concentration and activation polarizations [9, 10]. The concentration polarization may be attributed to the relatively low concentration (0.0245 M) of the depositable metal ions in the baths and the ability of the three metal ions to form  $M^{z+}$ -ammonium complex ions with various stability constants [11]. The activation polarization can be seen more clearly in Fig. 1b which shows that the Tafel relation holds good within the current density range 0.1–4.0  $A\ dm^{-2}$ . Moreover, as the concentration of  $Co^{2+}$  ion increases in baths 1 to 5, the polarization curves and the corresponding Tafel lines shift to less negative potentials. This may be attributed to the consequent decrease in the concentration and activation polarization of cobalt. This conclusion is supported by the fact that the stability constant of the  $Co^{2+}$ -ammonium complex ion ( $\log \beta_4 = 5.98$ ) is lower than that of the  $Ni^{2+}$ -ammonium complex ion ( $\log \beta_4 = 7.98$ ) [11]. A feature worthy of attention is that each of the Tafel lines shows an abrupt change in slope at a critical potential,

indicating a change in the mechanism of alloy deposition. However, the critical potential also shifts to less negative values with increasing concentration of  $Co^{2+}$  ion in baths 1 to 5.

To appraise the value of cathode potentials in explaining the mechanism of the alloy deposition, the polarization curves for the electrodeposition of individual cobalt, nickel and thallium metals from baths of similar composition to the alloy bath 4, except for the absence of the other depositable metal ions, were recorded and the results are shown graphically in Fig. 2a. The data reveal that the polarization curve of the alloy lies at less negative potentials than the curves of nickel and thallium, indicating ennobling of these two metals in co-deposition. However, many alloys show similar characteristics in their polarization curves during electrodeposition [5, 12]. The figure also shows that thallium is the least noble metal and this may be attributed to its extremely low concentration in the bath (0.001 M) beside the higher stability constant of the  $Tl^{+}$ -ammonium complex ion ( $\log \beta_4 = 13$ ) in comparison with the other two metal ion complexes [11].

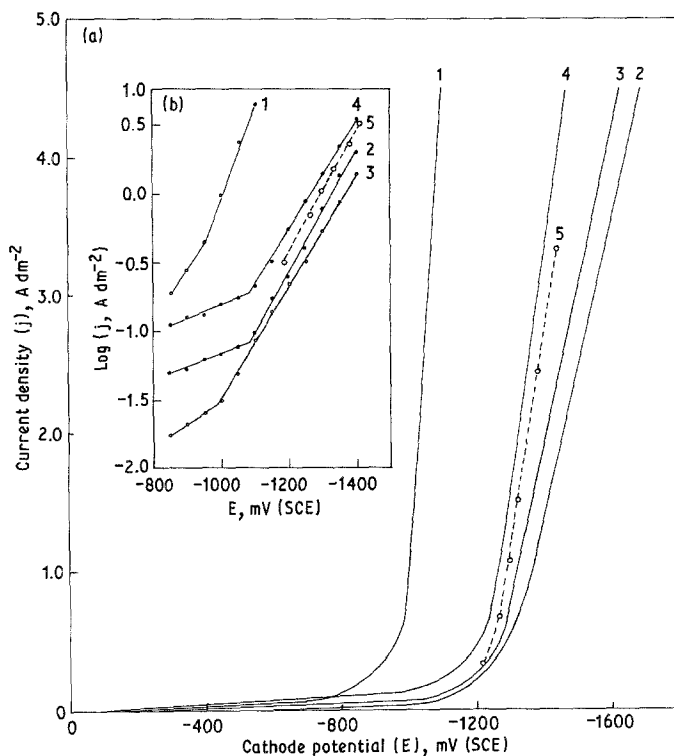


Fig. 2. (a) Polarization curves and (b) Tafel lines: (i) for electrodeposition of individual cobalt (curve 1), nickel (curve 2) and thallium (curve 3) metals and cobalt-nickel-thallium alloy from bath 4 (curve 4); (ii) calculated data for the discharge of  $H^+$  ions (curve 5) during electrodeposition of the alloy from bath 4.

Inspection of Fig. 2b reveals that along the lower branch of the Tafel relation for the alloy deposition (line 4), the electrodeposition of cobalt is attended by the least polarization (line 1). Therefore, it would be expected that cobalt deposits more readily in the alloy in this region. Along the upper branch of line 4, an increase in the current density causes the cathode potential to become more negative and hence the electrodeposition conditions approach more closely those represented by the less noble metals (lines 2 and 3). Accordingly, this increase in current density must be borne partly by an increase in the rate of deposition of the less noble metals in the alloy and partly by evolution of hydrogen. The first suggestion is confirmed by the observed increase in the metal-percentage of thallium (the least noble metal) in the alloy with increase of the deposition current density (see Section 3.2). Similarly, the second suggestion is supported by the observed decrease in the current efficiency of the alloy deposition with increase of the current density (see Section 3.3). Furthermore, the occurrence of an abrupt change in the slopes of the Tafel relations for

the individual metals (Fig. 2b) as well as for the ternary alloys (Figs 1b, 2b) also confirms the second suggestion. This feature could be ascribed to the co-deposition of  $H^+$  ions in all cases, especially at high current densities. Therefore, the polarization curve for the discharge of  $H^+$  ions in co-deposition with the alloy from bath 4 has been calculated by a previously reported method [13] and the data are shown plotted in Figs 2a and 2b.

### 3.2. Alloy composition

Fig. 3 shows the composition curves for cobalt, nickel and thallium in the alloy powders deposited from baths 1 to 5. The composition of the deposit is represented as a function of the metal-percentage of cobalt in the bath, although it could have been represented equally well as a function of the metal-percentage of nickel. The broken lines illustrate the composition reference lines representing the percentages of the three metals in baths 1 to 5. The data show that the percentage of either cobalt or nickel in the alloy increases with increase of its metal-percentage in

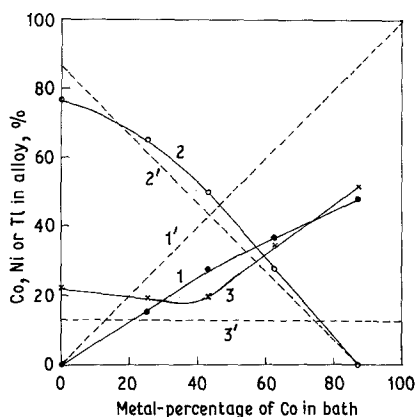


Fig. 3. Effect of the metal-percentage of cobalt in baths 1 to 5 on the percentages of cobalt (1), nickel (2) and thallium (3) in the alloy. The broken lines 1', 2' and 3' represent, respectively, the corresponding composition reference lines. Deposition current density ( $j$ )  $6.6 \text{ A dm}^{-2}$  and duration of electrolysis ( $t$ ) 10 min.

the bath. A marked feature of Fig. 3 is that the percentage of thallium in the deposit increases with increasing metal-percentage of cobalt in the bath. This could be referred to the corresponding overall depolarising effect during electro-deposition of the alloy (Fig. 1).

The relation of the least noble metal (thallium) to the other two metals is that of an anomalous alloy deposition system [14]. This is because the composition curve of thallium lies above its composition reference line indicating preferential deposition of thallium in the alloy. The relation between nickel and cobalt also seems to be that of anomalous co-deposition, since the composition curve of nickel lies slightly above its composition reference line whereas the

opposite is true with respect to the more noble metal (cobalt).

The advantage of triangular coordinates over rectangular coordinates in interpreting the data is that variations in the composition of either an electrodeposited ternary alloy or deposition bath is represented by one curve instead of three [12]. Unfortunately, most of the published data for ternary alloys have neither been based on a bath of constant total metal content nor represented by triangular coordinates. Therefore, the same data which are presented in Fig. 3 are reproduced in Fig. 4 in which the composition of the deposition baths is represented by line 1 and the composition of the alloys by curve 2. Tie-lines, represented by broken lines, are drawn from line 1 to curve 2 connecting the compositions of both the electrodeposited alloys and the corresponding baths. The upward direction of the tie-lines, with respect to the thallium key-line, shows that the deposits contain a larger percentage of thallium than in the bath. On rotating the figure so that the nickel key-line is horizontal, an inspection of the tie-lines also shows that the percentage of nickel in the deposit is higher than that in the bath. Therefore, both thallium and nickel are deposited preferentially. The left side of the alloy curve, 2, is almost parallel to the base of the triangle indicating that the percentage of thallium is nearly constant in this region, at about 20%. Another use of the tie-line is that its length is an indication of the divergence or similarity between the overall compositions of the alloy and the bath, expressed in percentage. For example, the tie-line  $ab$  is shorter than  $ef$  and this indicates that the percentage composition of the alloy is closer to the metal-percentages in the bath in the case of  $ab$  than  $ef$ .

The composition of the electrodeposited alloy from bath 4 was determined as a function of the deposition current density and the results are illustrated in Fig. 5. This figure shows also the composition reference lines of the three metals in bath 4 as dotted lines. The curves of Fig. 5 show that the percentages of cobalt and nickel in the deposit decrease and that of thallium increases with increase of current density. This may be ascribed to the fact that an increase in current density causes the cathode potential for the alloy

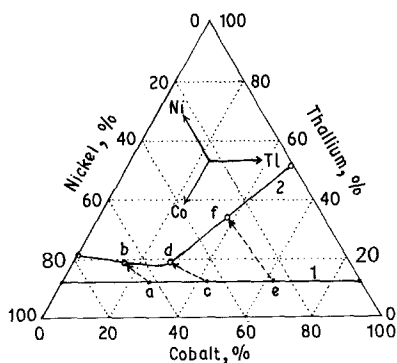


Fig. 4. Triangular coordinate representation of the relation between composition of baths 1 to 5 (line 1) and composition of the electrodeposited alloy powders (curve 2). The broken lines  $ab$ ,  $cd$  and  $ef$  are tie-lines;  $j = 6.6 \text{ A dm}^{-2}$ ;  $t = 10 \text{ min}$ .

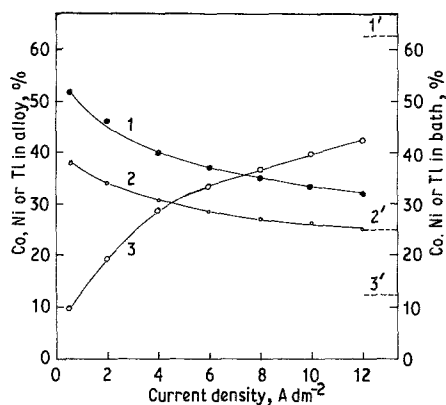


Fig. 5. Effect of current density on the percentages of cobalt (1), nickel (2) and thallium (3) in the alloy deposit from bath 4;  $t = 10$  min. The broken lines 1', 2' and 3' represent respectively the corresponding composition reference lines.

deposition to become more negative and accordingly the deposition conditions become more close to those represented by the polarization curve of the less noble metal (Fig. 2). This should increase the proportion of the less noble metal in the alloy. A comparison between the composition curves of cobalt, nickel and thallium and their corresponding composition reference lines confirms the above mentioned anomalous phenomenon of cobalt-nickel-thallium alloy deposition.

### 3.3. Current efficiency

The percentage cathodic current efficiency ( $f$ ) of

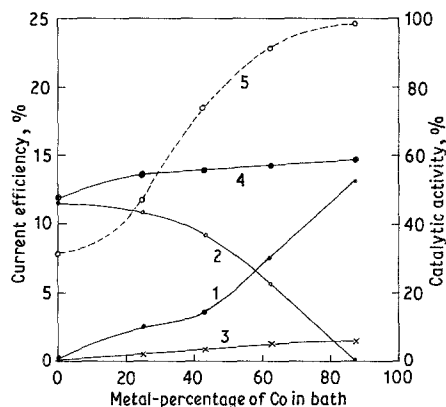


Fig. 6. Effect of the metal-percentage of cobalt in baths 1 to 5 on the partial current efficiencies of cobalt (1), nickel (2) and thallium (3) as well as the current efficiency of the alloy (4). The broken curve (5) represents the effect of the metal-percentage of cobalt in baths 1 to 5 on the catalytic activity of the alloy powder;  $j = 6.6 \text{ A dm}^{-2}$ ;  $t = 10$  min.

the alloy deposition from baths 1 to 5, as well as the partial efficiencies of the constituent metals, were determined and the results are represented in Fig. 6 as a function of the metal-percentage of cobalt in the bath. The figure shows that the partial  $f$  of cobalt increases gradually as its content in the bath increases, whereas that of nickel decreases in an opposite manner. This result may be explained on the basis that increasing the content of a metal in the bath increases its deposition efficiency through the corresponding decrease in the concentration polarization at the cathode [10]. In contrast, both the partial  $f$  of thallium and the  $f$  of the alloy increase slightly with increase of the metal-percentage of cobalt in the bath. This characteristic seems to be the sum of the opposing changes in the partial  $f$  of cobalt and nickel in addition to the slight improvement in the overall  $f$  of the alloy as a result of the corresponding ennobling of the polarization curve of the alloy deposition (Fig. 1). In general, the  $f$  of the alloy deposition from the baths examined is relatively low ( $\leq 15\%$ ) and this may be attributed to the low concentration of the depositable metal ions in the bath and the relatively high polarization accompanied by the deposition process (Fig. 1). Under this condition, hydrogen is discharged preferentially giving rise to a lower  $f$  of the alloy. Nevertheless, the  $f$  of the alloy is higher than the individual  $f$  of either thallium (6.6%), nickel (7.2%) or cobalt (10.6%) deposition from baths of similar composition and under identical operating conditions [1, 4, 7].

Fig. 7 shows a gradual decrease approaching a steady state for both  $f$  of the alloy deposition from bath 4 and the corresponding partial  $f$  of cobalt and nickel with increase of the deposition current density. This trend may be attributed to the observed increase in the cathodic polarization (Fig. 2) and the expected depletion of the noble depositable metal ions in the cathode layer with increase of current density. The latter factor is more effective during electrodeposition from a dilute solution such as the one used in the present study [6]. Accordingly, this improves the conditions for electrodeposition of the least noble metal (thallium) to some extent and evolution of hydrogen which consequently causes a decrease in  $f$  of the alloy deposition.

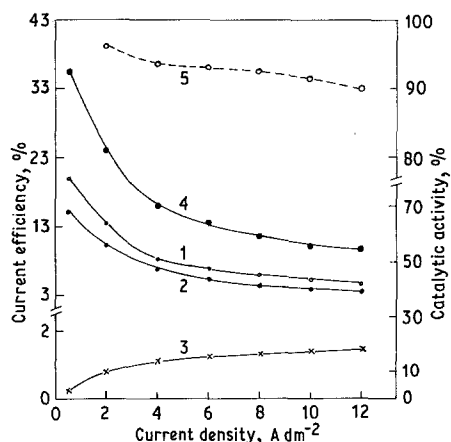


Fig. 7. Effect of current density on the partial efficiencies of cobalt (1), nickel (2), and thallium (3) as well as the current efficiency of the alloy (4). The broken curve (5) represents effect of the current density on the catalytic activity of the alloy powder from bath 4;  $t = 10$  min.

### 3.4. Surface morphology

The morphology of the as-deposited alloy powders from baths 1 to 5 was examined. Fig. 8 shows some of the electron micrographs which

depict the general trends of the morphological changes exerted by variation of the bath composition.

As can be seen in Fig. 8a, the nickel–thallium alloy powder from bath 1 forms in nodular-shaped dendrites almost covering the whole surface of the cathode. The inclusion of a small concentration of  $\text{Co}^{2+}$  ion in bath 2 leads to a modification of the growth morphology, of the nickel–thallium alloy, and formation of disperse leaf-like dendritic clusters of cobalt–nickel–thallium alloy powder (Fig. 8b). On increasing the concentration of  $\text{Co}^{2+}$  ion in baths 2 to 4, gradual increase of the particle size is observed (Fig. 8b, c). This feature may be correlated with the corresponding decrease in the cathodic polarization of the alloy deposition (Fig. 1). Such a condition favours enlargement of the particle size of the deposit rather than enhancement of the nucleation density [15, 16]. On the other hand, the cobalt–thallium alloy powder from bath 5 consists of elongated dihedral grains leaving some holes between them and oriented at random (Fig. 8d). The observed growth habit modifications may be referred to the specific

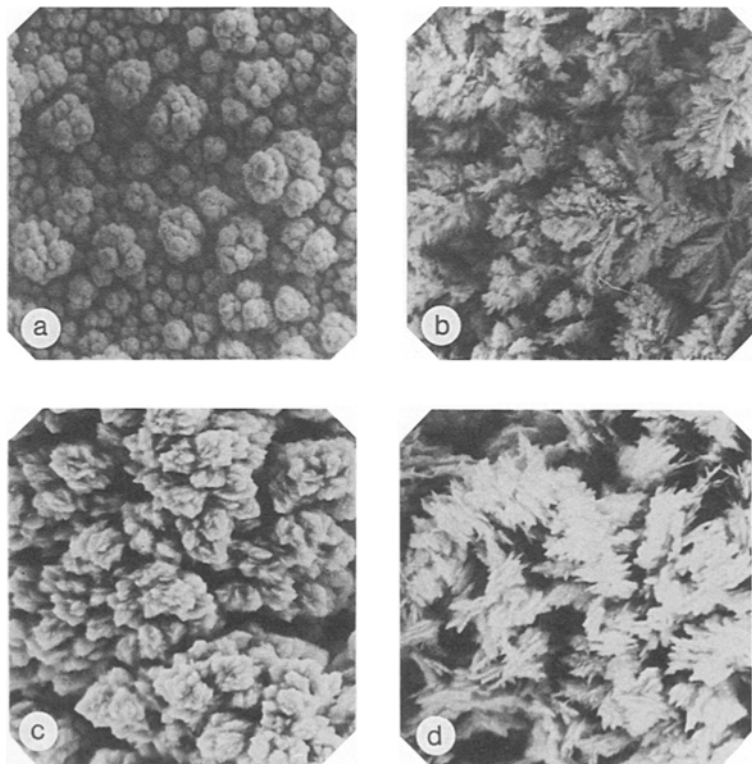


Fig. 8. Electron micrographs of electrodeposited alloy powders from: (a) bath 1, (b) bath 2, (c) bath 4 and (d) bath 5;  $j = 6.6 \text{ A dm}^{-2}$ ,  $t = 10$  min.  $\times 3850$ .

properties of the constituent metals of each alloy. In addition, the morphological shape of the ternary alloy (Fig. 8b, c) seems to be a combination of the shapes of the other two binary alloys (Fig. 8a, d).

### 3.5. Catalytic activity

The catalytic activity ( $D$ ) of the as-deposited alloy powders from baths 1 to 5 was measured and the results are shown graphically in Fig. 6 (curve 5) as a function of the metal-percentage of cobalt in the bath.

In general, the catalytic activity of the nickel-thallium alloy powder from bath 1 is relatively low (31%) whereas that of the cobalt-thallium alloy powder from bath 5 is almost 100%. This could be due to the corresponding decrease in the particle size of the alloy powder (Fig. 8a, d). However, the approximate increase of the surface area, and hence the catalytic activity, with decrease of particle size is expected [17, 18]. Moreover, it is observed that the catalytic activity of the cobalt-nickel-thallium alloy powders from baths 2 to 4 is in between those of the other two binary alloys and increases rapidly with increasing the metal-percentage of cobalt in the bath. These results indicate that there is a consistent dependence of the catalytic activity of an alloy on its composition. Since the morphology of an alloy powder is controlled by the alloy composition (Fig 8a-d), it can also be concluded that the catalytic activity of an alloy powder is a morphology-sensitive property. Similar conclu-

sions were reported for electrodeposited nickel [4], cobalt [7] and nickel-thallium alloy [6] powders.

Inspection of curve 1 (in Fig. 3) and curve 5 (in Fig. 6) depicts a rough parallelism between the percentage of cobalt in the alloy powder and the catalytic activity. A similar relationship was observed for cobalt-nickel alloy powders [8]. These results are in agreement with the fact that the catalytic activity of cobalt powder, electrodeposited from a bath of similar composition to bath 4, is relatively high ( $\approx 90\%$ ) and this seems to be a specific property of cobalt [7].

Fig. 7 (curve 5) shows a slight decrease in the catalytic activity of the cobalt-nickel-thallium alloy powder from bath 4 with increasing deposition current density. This result may be correlated with the corresponding decrease in the percentage of cobalt in the alloy powder (Fig. 5, curve 1) and this confirms the above discussion.

### 3.6. X-ray diffractometry

X-ray diffraction patterns of the alloy powders electrodeposited from baths 1 to 5 were determined and some representative results are included in Table 2. As can be seen in this table, the structure of an electrodeposited alloy is controlled by its percentage metal composition. For example, the nickel-rich alloy powder (sample I) is deposited in the face-centred cubic (fcc) structure and consists of only a single nickel-rich phase with orientations (111) and (200). In addition, the data show a slight increase in the

Table 2. Characteristics of X-ray diffraction patterns of cobalt-nickel-thallium alloy powders electrodeposited at  $j = 6.6 \text{ A dm}^{-2}$  and  $t = 10 \text{ min}$ . Sample I deposited from bath 2 and contains 65.37% nickel, 15.20% cobalt and 19.42% thallium. Sample II deposited from bath 4 and contains 28.19% nickel, 37.00% cobalt and 34.81% thallium

Sample number	Observed		Phases		hkl	Lattice parameters ( $\text{\AA}$ )			
	d ( $\text{\AA}$ )	I/I <sub>0</sub>	fcc	hcp		Observed		Standard	
						a	c	a	c
I	2.0364	100	Ni	-	111	3.5271	-	3.5238	-
	1.7641	36	Ni	-	200	3.5282	-	3.5238	-
II	2.1169	13	-	$\alpha$ -Co	100	2.5021	4.1088	2.5070	4.0700
	2.0390	100	Ni	-	111	3.5316	-	3.5238	-
	1.9167	15	-	$\alpha$ -Co	101	2.5021	4.1088	2.5070	4.0700
	1.7711	24	Co	-	200	3.5422	-	3.5447	-



lattice parameter  $a$  of the matrix metal (nickel) by the presence of the substitutional cobalt and thallium metals. This indicates the formation of cobalt–nickel–thallium solid solutions [5, 19].

The electrodeposited alloy powder in the intermediate range of alloy composition (sample II) consists of a mixture represented mainly by the face-centred cubic nickel-rich phase and minor proportions of face-centred cubic cobalt-rich and hexagonal close-packed (hcp)  $\alpha$ -cobalt-rich phases. Furthermore, the lattice parameters  $a$  and  $c$  of the matrix metal, corresponding to each alloy phase, change to a different extent by the coexistence of the other metals. These results are in good agreement with those reported in previous studies of cobalt–nickel alloys [8, 20]. Despite the appreciable metal-percentage (34.81%) of thallium in sample II, the X-ray examination did not detect the presence of any thallium-rich phase in the alloy. This may be attributed to the relatively higher atomic weight of thallium in comparison with that of cobalt or nickel ( $\approx 3.5:1$ ). Therefore, in this case the metal-percentage is not a good indication for the actual percentage number of atoms corresponding to each metal in the alloy, which was calculated and found to decrease in the order: cobalt (49.11%) > nickel (37.56%) > thallium (13.32%). Accordingly, it is probable that the number of thallium atoms in a matrix is not sufficient for its diffraction pattern to be distinct, and consequently it could not be recognized against the patterns of cobalt and nickel.

#### 4. Conclusions

The electrodeposition of fine-grained dendritic cobalt–nickel–thallium alloy powders would be feasible from dilute metal sulphate baths within the range found in some industrial effluents. Under the examined conditions the alloy powders deposit in the form of solid solutions and the phase structure is influenced by the percentage composition of each alloy. The catalytic activity of the alloy powders is a morphology-

sensitive property and increases with increase in the percentage of cobalt in the alloy. The composition of bath 4 may be considered optimum for electrodeposition of cobalt–nickel–thallium alloy powder characterized by a catalytic activity of 92% with a current efficiency of 14%, at deposition current density  $j = 6.6 \text{ A dm}^{-2}$  and  $t = 10 \text{ min}$ . The relatively low current efficiency of the alloy is a common feature in metal and alloy powder electrodeposition. Nevertheless, it is higher than those observed for electrodeposition of individual thallium (6.6%), nickel (7.2%) or cobalt (10.6%) metal powders from similar baths and under identical operating conditions.

#### References

- [1] A. M. Abd El-Halim and R. M. Khalil, *Surf. Technol.* **23** (1984) 215.
- [2] S. Wakabayashi, A. Murata and N. Wakabayashi, *Plat. Surf. Finish.* **69** (1982) 63.
- [3] A. M. Abd El-Halim, A. O. Baghalaf and R. M. Khalil, *Powder Technol.* **43** (1985) 103.
- [4] A. M. Abd El-Halim and R. M. Khalil, *Surf. Technol.* **26** (1985) 343.
- [5] *Idem*, *J. Appl. Electrochem.* **15** (1985) 217.
- [6] *Idem*, *J. Chem. Tech. Biotechnol.* **35** (1985) 407.
- [7] *Idem*, *Bull. Chem. Soc. Jap.* **58** (1985) 3555.
- [8] *Idem*, *Surf. and Coat. Technol.* **27** (1986) 103.
- [9] T. Yannakopoulos and A. Brenner, *J. Electrochem. Soc.* **103** (1958) 521.
- [10] A. M. Abd El-Halim, *J. Appl. Electrochem.* **14** (1984) 587.
- [11] L. G. Sillen and A. E. Martell, 'Stability Constants of Metal Ion Complexes', Chemical Society, London (1971) p. 84.
- [12] A. Brenner, 'Electrodeposition of Alloys', Vol. I, Academic Press, New York (1963) pp. 114, 343–50.
- [13] A. M. Abd El-Halim, *Surf. Technol.* **23** (1984) 207.
- [14] A. Brenner, 'Electrodeposition of Alloys', Vol. II, Academic Press, New York (1963) p. 297.
- [15] S. Itoh, N. Yamazoe and T. Seiyama, *Surf. Technol.* **5** (1977) 27.
- [16] A. M. Abd El-Halim and M. I. Sobahi, *ibid.* **19** (1983) 45.
- [17] K. Appelt, Z. Dominiczak, A. Nowaki and M. Paszhiewicz, *Electrochim. Acta* **10** (1965) 617.
- [18] I. F. Hewaidy, H. O. Sabra and E. H. Nassif, *Powder Technol.* **24** (1979) 245.
- [19] S. S. Abd El Rehim, A. M. Abd El-Halim and M. M. Osman, *J. Appl. Electrochem.* **15** (1985) 107.
- [20] *Idem*, *J. Chem. Tech. Biotechnol.* **35** (1985) 415.